



Characterization of microbial current production as a function of microbe–electrode–interaction



Kerstin Dolch^a, Joana Danzer^b, Tobias Kabbeck^a, Benedikt Bierer^b, Johannes Erben^b, Andreas H. Förster^a, Jan Maisch^c, Peter Nick^c, Sven Kerzenmacher^b, Johannes Gescher^{a,*}

^a Institute for Applied Biosciences, Department of Applied Biology, Karlsruhe Institute of Technology, Fritz-Haber-Weg 2, 76131 Karlsruhe, Germany

^b Laboratory for MEMS Applications, IMTEK – Department of Microsystems Engineering, University of Freiburg, Georges-Koehler-Allee 103, 79110 Freiburg, Germany

^c Botanical Institute, Molecular Cell Biology, Karlsruhe Institute of Technology, Kaiserstrasse 2, 76131 Karlsruhe, Germany

HIGHLIGHTS

- Biological and electrochemical analysis of MFC anode material performance.
- Evaluation of a correlation between population and current density.
- Comparison of pure and mixed cultures as biological catalysts.
- Effect of co-culturing on biofilm formation and current production.
- Detailed comparison of *S. oneidensis* and *G. sulfurreducens* MFC performance.

ARTICLE INFO

Article history:

Received 28 November 2013

Received in revised form 24 January 2014

Accepted 27 January 2014

Available online 4 February 2014

Keywords:

Microbial fuel cell

Shewanella oneidensis

Geobacter sulfurreducens

Electrode material

qPCR

ABSTRACT

Microbe–electrode–interactions are keys for microbial fuel cell technology. Nevertheless, standard measurement routines to analyze the interplay of microbial physiology and material characteristics have not been introduced yet. In this study, graphite anodes with varying surface properties were evaluated using pure cultures of *Shewanella oneidensis* and *Geobacter sulfurreducens*, as well as defined and undefined mixed cultures. The evaluation routine consisted of a galvanostatic period, a current sweep and an evaluation of population density. The results show that surface area correlates only to a certain extent with population density and anode performance. Furthermore, the study highlights a strain-specific microbe–electrode–interaction, which is affected by the introduction of another microorganism. Moreover, evidence is provided for the possibility of translating results from pure culture to undefined mixed species experiments. This is the first study on microbe–electrode–interaction that systematically integrates and compares electrochemical and biological data.

© 2014 Elsevier Ltd. All rights reserved.

1. Introduction

A number of microorganisms are able to transport electrons from the cell surface to an insoluble electron acceptor. This respiratory mechanism has most probably evolved to respire on insoluble minerals like hematite, ferrihydrite or birnessite in anoxic soils or sediments. The low specificity of the electron transfer processes

allows for the bioengineering of exhaustless insoluble electron acceptors in the form of anode materials that can be embedded in microbial fuel cells (MFCs). These MFCs contain anodes to which microbes transfer catabolic electrons, and cathodes at which electrons are transferred to a terminal electron acceptor. The applied research on MFCs progresses in various directions including the integration of anodes in the waste water treatment process as a tool for carbon elimination or in bioreactors as an enabling technology for unbalanced fermentations (Flynn et al., 2010).

All MFC applications share the necessity to establish optimal microbe–electrode–interactions allowing for high turnover rates and the construction of low-priced MFCs. A key to reduce costs is the introduction of cost-efficient electrode materials that can be produced in large quantities. A number of publications describe the usage of carbon materials with different configurations

* Corresponding author. Tel.: +49 721 608 41940; fax: +49 721 608 41941.

E-mail addresses: kerstin.dolch@kit.edu (K. Dolch), joana.danzer@imtek.uni-freiburg.de (J. Danzer), Kabbeck@gmx.de (T. Kabbeck), bbierer@web.de (B. Bierer), johannes.erben@imtek.uni-freiburg.de (J. Erben), andreas.foerster@kit.edu (A.H. Förster), jan.maisch@kit.edu (J. Maisch), peter.nick@kit.edu (P. Nick), kerzenma@imtek.uni-freiburg.de (S. Kerzenmacher), johannes.gescher@kit.edu (J. Gescher).

including carbon paper, cloth, felt, mesh or brushes. However, a systematic comparison of materials with different characteristics is mostly lacking and it is not possible to compare current densities from different studies since the experiments were mostly not conducted under similar conditions (Logan, 2009). Furthermore, the biological context has only been rarely considered. The use of MFCs for applied processes demands stable microbe–electrode–interactions. This is particularly important since most applications will require hydrodynamic flow to provide substrates or to remove products. Hence, stable biofilms of exoelectrogenic microorganisms are necessary. This aspect of biofilm formation as key for anode performance has been mostly overlooked. Therefore, a systematic characterization of microbe–electrode–interaction and the impact of this interaction on the performance of MFCs was conducted. Strains and anode materials were compared using a measurement routine that was based on (I) the time that the microbes needed to establish a constant anode potential in an initial galvanostatic step and (II) the ability of the microbes to sustain a current gradient. The results were correlated with the density of biological material on the anodes. *Geobacter sulfurreducens* was superior over *Shewanella oneidensis* in anode reduction although it reduced under the tested conditions ferric citrate slower. The specific surface of the materials was key to anode performance but did not linearly correlate to limiting current densities. Interestingly, the biofilm behavior of the organisms changed in mixed species experiments. Last but not least, this study provides evidence for the possibility to choose a suitable anode material for field applications by using laboratory experiments with pure cultures of exoelectrogenic organisms.

2. Methods

2.1. Bacterial strains and growth conditions

S. oneidensis MR-1 and *G. sulfurreducens* PCA (DSM12127) were cultured at 30 °C in a minimal medium which was developed based on compositions published by Coppi et al. (2001) and Holmes et al. (2004). The medium contained 3 mM KH₂PO₄, 1 mM K₂HPO₄, 4 mM NH₄Cl, 5 mM KCl, 6 mM NaCl, 1 mM MgCl₂, 21 mM HCO₃Na, 5 mM CO₃Na₂, 20 mM sodium lactate, 10 mM sodium acetate, 0.2 mM of sodium ascorbate, 5.1 mM CaCl₂, 10 ml of NB trace mineral solution (Coppi et al., 2001), 1.0 ml selenite–tungstate solution [13 mM NaOH, 17 μM Na₂SeO₃, and 12 μM Na₂WO₄], 10 ml vitamin solution (German Type Culture Collection, DSMZ, media 141), 0.1% (w/v) yeast extract, and 1 mM cysteine. Prior to autoclaving, all anoxic media were boiled and thereafter purged from oxygen for 30 min with a mixture of 80% N₂/20% CO₂. Thereafter, pH was adjusted to 7.2. For comparative growth experiments, 40 mM ferric citrate was added as electron acceptor. Prior to MFC experiments, microbial strains were pre-grown in the above described minimal medium containing 40 mM disodium fumarate, 10 mM NaNO₃, and 1 mM ferric citrate. No electron acceptors were added to the medium in MFC experiments.

2.2. MFC setup and electrochemical measurements

MFCs were operated in a two-chamber setup adapted from previous work (Kloke et al., 2010) (Fig. A1). A Fumapem F-950 membrane (Quintech, Göppingen, Germany) was used to separate the anode chamber from a saturated calomel reference electrode (SCE) (Sensortechnik Meinsberg GmbH, Ziegra-Knobelsdorf, Germany) and the cathode chamber, which was filled with 25 ml of buffer containing 3 mM KH₂PO₄, 1 mM K₂HPO₄, 4 mM NH₄Cl, 5 mM KCl, 68 mM NaCl, 1 mM MgCl₂, 10 ml of NB trace mineral solution, 1.0 ml selenite–tungstate solution, and 0.2 mM sodium

ascorbate. Cathodes were continuously purged with air. Potentials measured at the working electrode against SCE were converted to normal hydrogen electrode (NHE) potentials by addition of 241 mV. The anode chamber was filled with 25 ml of anoxic minimal medium. The whole compartment was flushed continuously with an 80% N₂/20% CO₂ mixture to maintain a constant anoxic environment with a stable pH. The optical density of the bacterial culture was measured at 655 nm, and the starting cell density in the anodic chamber was 0.3. Lactate (0.4 mmol) was added to MFCs inoculated with *S. oneidensis* every 48 h to avoid limitations of electron donors. All MFC experiments were conducted at least in independent triplicates and at a constant temperature of 30 °C.

Three different materials were tested as anodes. Graphite foil (0.254 mm thick) was purchased from Alfa Aesar (Karlsruhe, Germany), graphite felt GFD2 EA (2 mm thick) from SGL Group, Carbon Company (Meitingen, Germany), and activated carbon cloth C-Tex 13 from Mast Carbon International Ltd. (Hampshire, United Kingdom). Material characteristics are described in detail in Kipf et al. (2013). Prior to usage, the electrodes were first rinsed with isopropanol and thereafter autoclaved in deionized water. The electrodes were connected via platinum wires (0.1 mm; Chempur, Karlsruhe, Germany) to a potentiostat (Pine Instruments, Grove City, USA).

The standard measurement protocol was modified after Golitsch et al. (2013) and consisted of two phases. First, a constant current of 222.22 nA cm⁻² was applied in a galvanostatic conditioning period until the measured anode potential reached a stable value. In the second phase (current sweep phase), the current was constantly increased with a rate of 3.24 nA s⁻¹ cm⁻². Current densities at 41 mV vs. NHE were used to compare anode performance of the two organisms on the three tested materials.

2.3. Mixed sewage MFCs

MFCs inoculated with sewage sludge were operated similarly, differing only in inoculum and volume. The anode and cathode chambers were filled with 40 ml of the above-mentioned medium and inoculated with 1 ml of a 4:1 mixture of material from an anaerobic digester and activated sludge. Both were obtained from the municipal waste water treatment plant “Kläranlage Untere Elz” in Teningen, Germany. The electrochemical measurements were performed as described above using a potentiostat (1470E, Solartron Analytical, Farnborough, United Kingdom).

2.4. Measurement of electrode double-layer capacitance

The double-layer capacitance of the used electrodes was determined by running current sweeps without inoculation. Assuming, that close to the open circuit potential no faradaic current is produced, the measured potential drop can be related to the behavior of a (dis)charging capacitor according to:

$$\Delta U = \frac{1}{2vC} I^2 \quad (1)$$

Herein C is the capacity in Farad, v represents the current sweep rate in A s⁻¹, I is the current in Ampere, and ΔU the potential with respect to the open circuit potential in Volt. The electrodes capacitance can now be obtained using 3.24 nA s⁻¹ cm⁻² as sweep rate and fitting the function to the measured values for ΔU and I. ΔU was calculated as the difference between the open circuit potential and the measured potential during the current sweep.

The capacitance obtained for C-Tex 13 was measured in triplicate and is 3.56 F ± 0.29 F for the whole electrode (2.25 cm²). Calculated according to Kipf et al. (2013) the relative capacitance results in 12 μF cm⁻² BET surface.

Due to the much smaller specific surface of graphite felt and graphite foil, their capacitance is three orders of magnitude lower.

This renders the capacitive contribution to the total current almost negligible compared to the faradaic part. Nevertheless, measured average values of 6.9 mF for graphite felt and 12.6 mF for graphite foil were used for the correction.

2.5. Fluorescent *in situ* hybridization (FISH)

Whole anodes were fixed for 4 h at 4 °C in PBS buffer containing 4% formaldehyde. Thereafter, anodes were washed for 30 min at 4 °C in PBS and then treated with 80% and 70% ethanol for 1 min, respectively. To improve permeability, 0.1 M HCl were applied for 1 min and thereafter anodes were dried. Hybridizations were performed at 46 °C for 2 h in a moist atmosphere containing appropriate formamide concentrations (Table 1). The hybridization solution consisted of 5.4 mM HCl, 0.12 mM Tris–HCl, pH 8.0, 0.1% SDS, and appropriate concentrations of formamide. Furthermore, 6.67 pmol μl^{-1} fluorescently labeled oligonucleotides, and, if necessary, the same concentration of helper oligonucleotides were added (Table 1). Thereafter, the anodes were first rinsed with the washing solution, and then incubated for 15 min in the washing solution at 48 °C. This solution consisted of 1 mM Tris–HCl, pH 8.0, 0.25 mM EDTA pH 8.0, 0.1% SDS, and appropriate concentrations of NaCl (46 mM for *S. oneidensis* and 215 mM for *G. sulfurreducens* hybridizations, respectively). Thereafter, anodes were rinsed with deionized water and incubated for 15 min in SSC buffer [75 mM NaCl, 7.5 mM $\text{C}_6\text{H}_5\text{Na}_3\text{O}_7$, pH 6.0]. Afterwards, samples were dried at 37 °C and counterstained with SYTO 45 according to the manufacturer's instructions (Invitrogen, Darmstadt, Germany). Images were recorded by widefield fluorescence either at an AxioImager Z1 (Zeiss, Oberkochen, Germany) using a 40 \times water immersion lens and a cooled digital CCD camera (AxioCam MRm, Zeiss) or a Leica DM 5500 B microscope using a 63 \times water immersion lens and a DFC 300 FX digital color camera from Leica (Wetzlar, Germany). With the Zeiss microscope the filter sets 38 HE (excitation at 470 nm, beam splitter at 495 nm and emission at 525 nm), 43 HE (excitation at 550 nm, beam splitter at 570 nm and emission at 605 nm), and 47 HE (excitation at 436 nm, beam splitter at 455 nm and emission at 480 nm) were used for FITC, Cy3, and SYTO 45, respectively. For the Leica microscope, the filter sets L5 (excitation filter 480/40 and suppression filter 527/30) and Y3 (545/30 and 610/75) were used for FITC and Cy3, respectively. Picture-stacks were assembled using the software tool ImageJ (Rasband, 1997–2004).

2.6. Extraction of DNA

After completion of the MFC program, anodes were cut into two pieces and then DNA was extracted using the innuPREP Stool DNA Kit from Analytic Jena (Jena, Germany) according to the manufacturer's instruction. Standard curves were compiled with pure cultures. Therefore, the cells were first counted using a Neubauer counting chamber (Marienfeld, Lauda-Königshofen, Germany) and serial dilutions were prepared in triplicate. From each of the six dilution steps DNA was extracted according to the manufacturer's instructions.

2.7. Quantitative PCR (qPCR)

Strain-specific primers were designed with the software tool Beacon Designer (Premier Biosoft, Palo Alto, USA) to quantify the abundance of *S. oneidensis* and *G. sulfurreducens* in the anodic chambers via qPCR (Table 2). All qPCR reactions were developed in a CFX96 Cyclor (Bio-Rad, Munich, Germany) using white polypropylene thin-walled plates (4titude Wotton, United Kingdom) and adhesive qPCR seal (Sarstedt, Nümbrecht, Germany). The reaction volume of 20 μl was chosen according to the DyNamo Flash SYBR Green qPCR Kit manual (biozym, Hessisch Oldendorf, Germany). The primer concentration was 0.5 μM , and 1 μl of template-DNA was added. The optimal annealing temperature was determined with isolated DNA of the pure strains using a temperature gradient qPCR. All experiments were accompanied by no template controls. All qPCR reactions were verified on a 2.5% agarose gel.

Standard curves were established using biological triplicates and applied on each qPCR plate. On the basis of the standard curves, cell counts of each isolated DNA sample were determined. Cell quantifications of anode samples are based on at least three MFCs. As mentioned before, anodes were split in two pieces, which were independently used for DNA extraction. Hence, two DNA samples were generated per MFC. Quantitative PCR experiments with these samples were conducted in technical triplicates. The cell count per anode was gained by adding the cell count means of the two half anodes.

2.8. Analytical measurements and statistical analysis

Lactate and acetate concentrations were quantified via HPLC according to Kipf et al. (2013). Ferrous iron concentrations were determined according to Ruebush et al. (2006). Statistical analysis was conducted using SPSS (IBM, Ehningen, Germany). All data sets were normally distributed. An unpaired *t*-test was used to determine significance of the data. The level of significance was set to 5%.

3. Results and discussion

3.1. Establishing a growth medium

The main goal of this study was to analyze the performance of MFCs as a function of microbial activity and microbe–electrode–interaction. A byproduct of this analysis was a direct comparison of the two exoelectrogenic model organisms *S. oneidensis* and *G. sulfurreducens*. The first milestone that had to be reached was to establish one medium that would support growth of both organisms to a highly similar extent to circumvent artifacts caused by differential responses of the two model organisms to the medium. The bicarbonate buffered medium contained a mixture of lactate and acetate as carbon and electron sources. Reduction of ferric citrate was used as readout to assess growth. Ferric iron reduction rates varied to a minor extent between the two strains (Fig. 1). Of note, *S. oneidensis* was catalyzing extracellular electron transfer

Table 1
Fluorescently labeled oligonucleotide probes and helper oligonucleotides used for *in situ* hybridization experiments.

Probe	Target	Sequence (5'–3')	Specificity	Source or reference	FA [%]
SHEW227	16S rRNA	AGC TAA TCC CAC CTA GGT WCA TC	<i>Shewanella</i> spp.	Huggett et al. (2008)	40
Geo2	16S rRNA	GAA GAC AGG AGG CCC GAA A	<i>G. sulfurreducens</i>	Richter et al. (2007)	20
HGEO2-1	Helper probes for GEO2	GTC CCC CCC TTT TCC CGC AAG A		Richter et al. (2007)	
HGEO2-2	Helper probes for GEO2	CTA ATG GTA CGC GGA CTC ATC C		Richter et al. (2007)	

Table 2
Sequences of primers used for real-time PCR experiments.

Probe	Sequence (5'–3')	Usage
S.o. SYBR GREEN for	TAT TCA AGT GCT TCT ATT AG	Quantification of <i>S. oneidensis</i> cells
S.o. SYBR GREEN rev	AAG AAC TTC TAC TCA ACA	
G.s. SYBR GREEN for	TCT GGT TTA TGG AAG AAG TTT GG	Quantification of <i>G. sulfurreducens</i> cells
G.s. SYBR GREEN rev	TGT TAA AGG TCT GAT GTG TGA GA	

under these ferric iron-reducing conditions faster than *G. sulfurreducens* [1.28 ± 0.17 vs. 1.86 ± 0.25 mM $\text{Fe}^{2+} \text{h}^{-1}$].

Ferric citrate was added in concentrations (40 mM) that were limiting with respect to the abundance of electron donors. As expected, *S. oneidensis* used only lactate as carbon and energy source (Yoon et al., 2013). 10.9 ± 0.3 mM lactate were consumed and converted to 8.8 ± 0.2 mM acetate and biomass. This indicates an anabolic substrate usage of 2.1 mM, which equals to 19%. Concomitantly, 37 mM ferric citrate were reduced to Fe^{2+} , indicating a release of roughly 4 mol electrons per mol of catabolically consumed lactate. These electrons most probably stem from the oxidation of (I) lactate to pyruvate, and (II) formate to CO_2 (Scott and Neelson, 1994). Under the same conditions, *G. sulfurreducens* oxidized 5.1 ± 0.3 mM acetate and 2.7 ± 0.6 mM lactate. Without labeling studies it is neither possible to determine the primary electron donor nor to what extent it was used for the buildup of biomass or catabolism. However, it is known, that *G. sulfurreducens* can couple the reduction of ferric iron to the oxidation of acetate (Caccavo et al., 1994) and lactate (Call and Logan, 2011). What can be extracted from this data is, that *G. sulfurreducens* cells pre-adapted to this medium containing both electron donors, consumed lactate and acetate simultaneously.

Taking together, the established medium allowed reduction of a colloidal but cell-impermeable electron acceptor by *S. oneidensis* and *G. sulfurreducens* with similar rates, which was of outmost importance for following experiments.

3.2. Galvanostatic conditioning

MFC experiments were started by applying a constant but low current of $222.22 \text{ nA cm}^{-2}$ and the decrease of anode potential was followed over time. The time until a constant potential was

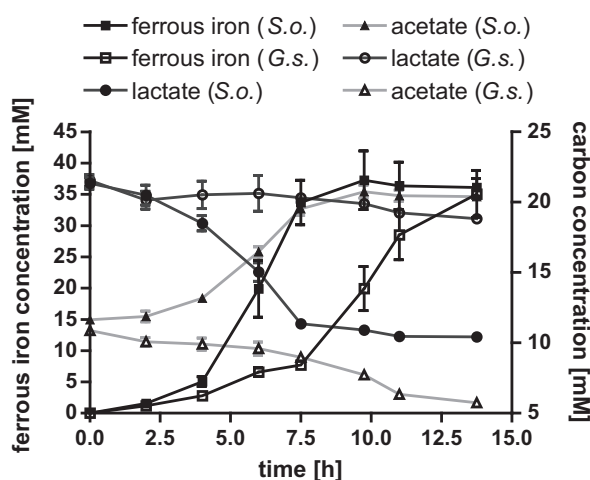


Fig. 1. Growth curves of *S. oneidensis* and *G. sulfurreducens* in the established basic anoxic medium. Experiments were conducted in quadruplicates. Error bars indicate standard deviation. Ferrous iron concentrations are indicated by squares. Circles and triangles show lactate and acetate concentrations, respectively. *S. oneidensis* data sets are indicated by closed symbols, whereas *G. sulfurreducens* data is marked by open symbols.

reached was referred to as *conditioning period*. Interestingly, this period varies with the tested anode materials as well as with the microbial strains used. These differences in length of the conditioning periods could reflect the ability of the cells to establish an initial and stable interaction with the electrode material. This interaction is most probably dependent on the capability of the cells to conduct electron transfer onto the anode surface as well as to some extent on their ability to establish a biofilm on the anode material. Biofilm formation will be more important for *G. sulfurreducens*, since previous studies established the necessity of direct contact between *Geobacter* cells and the insoluble electron acceptor (Nevin and Lovley, 2000). In contrast, growth of *S. oneidensis* under batch conditions leads to the release of flavin molecules that can be used as mediators for electron transfer between cell and anode surface (Marsili et al., 2008).

Three graphite based anode materials were tested that had been previously characterized in detail and show a large variation in terms of porosity and specific surface area (Kipf et al., 2013). On the macroscopic scale, graphite felt ($60 \text{ m}^2 \text{ g}^{-1}$) and C-Tex 13 ($800 \text{ m}^2 \text{ g}^{-1}$) comprise fabrics of varying three dimensional properties, while graphite foil can be approximated as a two dimensional material. As indicated in Fig. 2, the two tested organisms show an extreme variation in the conditioning period. On graphite foil, *S. oneidensis* needs 162 h to establish a potential of -97 mV, while *G. sulfurreducens* cells need only 8 h to trigger the potential to a thereafter constant value of -229 mV. From all three materials tested, graphite felt seems to be the most suitable for an interaction with *S. oneidensis*. Within 33 h, the potential of the anode dropped to -210 mV, which is close to the -241 mV that can be gained in MFCs inoculated with *G. sulfurreducens* in 11 h. On C-Tex 13, the material with the highest surface per weight ratio, *Geobacter* cells establish within 17 h a potential of -238 mV and are thereby 10 times faster compared to *S. oneidensis*. Nevertheless, *Shewanella* cells at least lowered the anode potential to -234 mV.

The final potential of the conditioning period will be dependent on the redox potential of the enzymes or shuttles that conduct terminal electron transfer. Outer membrane cytochromes expressed by both organisms under anode reducing conditions as well as flavins have midpoint or redox potentials within this range (Marsili et al., 2008; Hartshorne et al., 2007; Lloyd et al., 2003). Along these lines, it is interesting to note that *S. oneidensis* was not capable of adjusting the anode potential to values below -200 mV if graphite foil was used as electron acceptor. This could be due to the surface properties that might prevent sufficient biofilm formation. Alternatively, there is evidence for a function of released flavin molecules as electron shuttles (Marsili et al., 2008). Hence, the reduced hyperpolarization of the anode could indicate that the interaction of flavins with the material might also be hampered.

It was expected that the coverage of anodes with cells in conjunction with the electrodes double-layer capacitance would play an important role for the duration of the conditioning period. Hence, increased surface area should result in longer conditioning times. With exception of the interaction between graphite foil and *S. oneidensis*, indeed conditioning times rise with material surface area. Nevertheless, at least for *Geobacter*, the differences in conditioning time do not directly reflect the differences in surface area of the materials that are by far more pronounced. This is most

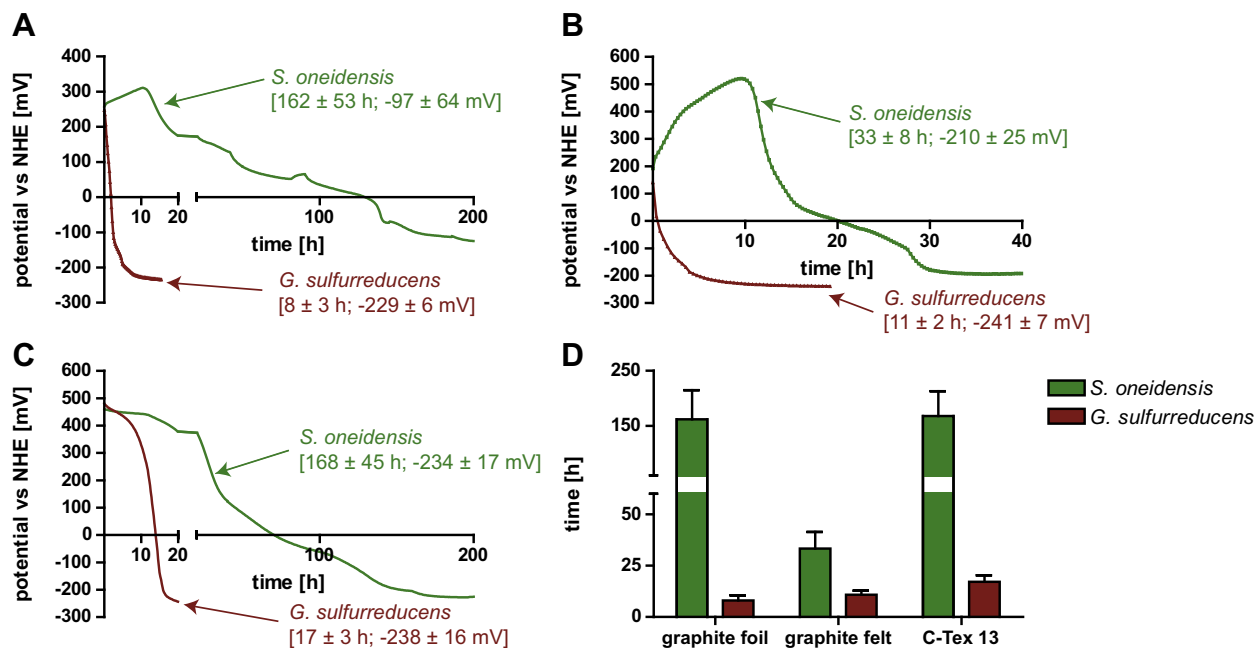


Fig. 2. Galvanostatic conditioning. Conditioning periods at $222.22 \text{ nA cm}^{-2}$ for *S. oneidensis* (green) and *G. sulfurreducens* (red). Graphs show one example of the six independently conducted experiments. Numbers indicate average conditioning period duration and final potentials. Standard deviations are given. (A) Graphite foil, (B) graphite felt, and (C) C-Text 13. (D) Overview of the time needed for establishing a constant potential for each material and strain.

probably due to the fact that only a certain amount of the material is accessible for the bacterium while a large proportion will be buried within the fabric. This part is not only inaccessible but most probably even insulated from the surrounding medium by the bacterial biofilm. Compared to *G. sulfurreducens*, *S. oneidensis* shows more prominent differences in conditioning time between graphite felt and C-Text 13. As will be shown in Section 3.4, coverage of the material with *S. oneidensis* biofilms is rather low. Hence, shuttling compounds will most probably be important for electron transfer. This was also shown in previous reports in which it was concluded that 70% of the *S. oneidensis* electron transfer to anode surfaces is been conducted by flavin molecules that shuttle electrons between planktonic cells and the anode (Marsili et al., 2008). Hence, in contrast to what was mentioned regarding the interaction of *G. sulfurreducens* with the anode materials, *S. oneidensis* is not able to cover the surface confluent and more anode material will be available for the small shuttling compounds. This might explain why the conditioning period of *S. oneidensis* on C-Text 13 is five times as long as on graphite felt.

In conclusion, although *S. oneidensis* shows faster ferric iron reduction in the established growth medium, *G. sulfurreducens* is able to adapt faster to the reducing conditions at the anode.

3.3. Current sweep experiments

Current sweep experiments were conducted as a second step following the conditioning period. Thereby, it was possible to observe changes of anode potential as a function of applied current density starting from one homogenous starting potential. MFCs with *S. oneidensis* inoculated graphite foil showed a more positive starting potential and certainly represent the exception. Besides a similar initial starting point regarding the anode potential, it was thereby also possible to compare the respiratory electron transfer rates irrespective of potential initial limitations or differences of microbe–electrode-interactions. Current densities determined at a potential of 41 mV were used to compare the performance of the two strains on the three materials. This value was chosen since MFCs inoculated with the two strains did not show uniform curve

progression and since the results were best comparable at this value (Fig. 3). At a certain point, all curves migrate with steep slopes to potentials higher than 1 V, which is due to abiotic water cleavage on the anodes to sustain the current draw. At lower current densities, *G. sulfurreducens* exhibit slower electrode polarization compared to *S. oneidensis*. One potential reason for this difference could be that *S. oneidensis* cells conduct electron transfer mostly via electron shuttles. Hence, the traveling distance for the electrons will be longer, which results in higher polarization losses. In contrary, the only mode of electron transfer for *G. sulfurreducens* is direct contact, which is more efficient and hence resulting in lower polarization. Especially when using high surface materials as C-Text 13, capacitive current can account for a large proportion of the performance. To make sure, that performance is clearly related to microbial activity and not to the discharging of a capacitor, obtained polarization curves were corrected from the contribution of the double-layer capacitance of the materials by subtracting the capacitive current according to Eq. (1).

For both strains, a connection between available surface area and current density is evident. *S. oneidensis*, as well as *G. sulfurreducens* showed ascending performance from graphite foil over graphite felt to C-Text 13. Apparently, the area of available surface determines to a certain extent the number of electron transfer processes per time. In all cases, *Geobacter* cells sustained current densities that were 4–7.3 times higher compared to *S. oneidensis*. It should also be mentioned that the amount of residual substrates was quantified after each current sweep experiment using HPLC analysis. These experiments indicated that electron donor limitation was not observable during the current sweeps (data not shown).

3.4. Anode population

So far, the conducted MFC experiments lead to electrochemical data, but do not provide sufficient evidence to conclude whether population density on anodes is the limiting factor for MFC performance, or whether the ability of the cells to conduct electron transfer onto the anodes might also vary between different

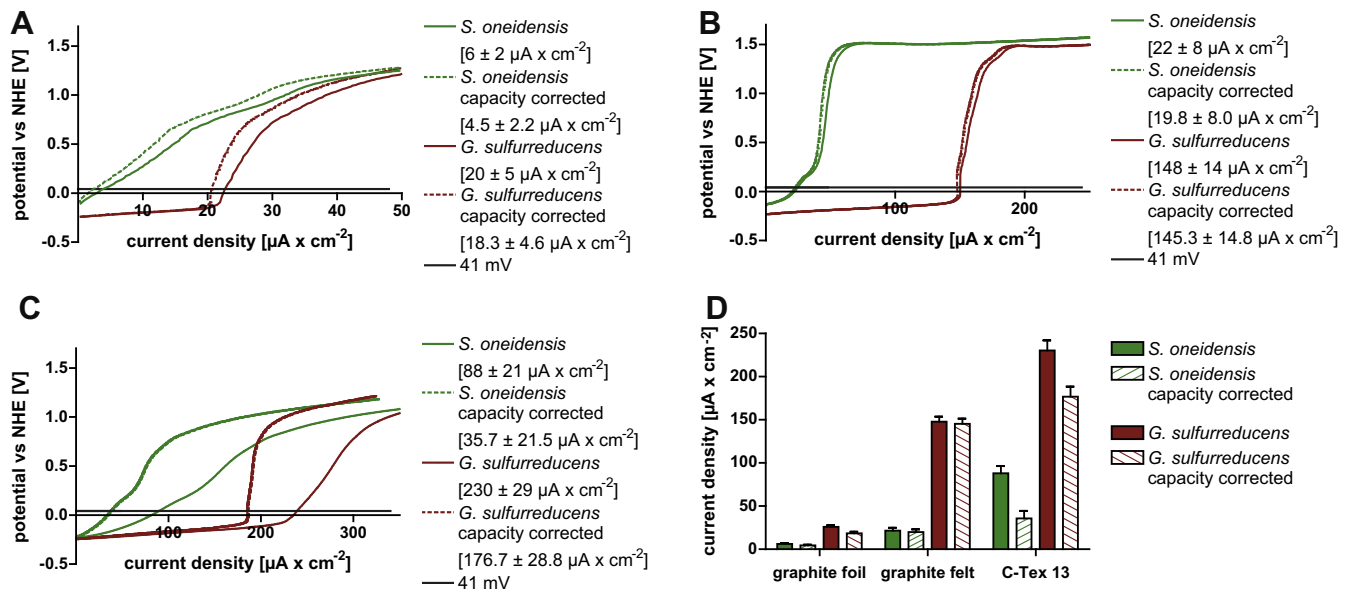


Fig. 3. Current sweep experiments. Current sweep experiments with ascending currents of $3.24 \text{ nA s}^{-1} \text{ cm}^{-2}$ for *S. oneidensis* (green) and *G. sulfurreducens* (red). Graphs show one example of the six independently conducted experiments. Numbers indicate average current density values at 41 mV. Standard deviations are given. Dashed lines indicate capacitance corrected curves. (A) Graphite foil, (B) graphite felt, and (C) C-Tex 13. (D) Comparison of the current densities at 41 mV. Capacitance corrected values are marked with stripes.

carbon-based anode materials. Hence, the population density after current sweep experiments was assessed using two independent methods. As suggested by Yates et al., PCR dependent and independent analyses were used concomitantly to avoid artifacts (Yates et al., 2012). First, FISH was conducted. In previous studies, the anodic population was visualized by embedding whole anodes in a matrix for subsequent cryostat sectioning (Okabe et al., 1999). In the current study, a new protocol was established, that circumvents time consuming and artifact-prone embedding and slicing. As indicated in Fig. A2A–F, it is obvious that the amount of *G. sulfurreducens* cells on the anode surfaces increases in the order graphite foil, graphite felt, C-Tex 13. Hence, the material with the highest surface area seems to be colonized with the highest amount of cells. Overall, *G. sulfurreducens* forms denser biofilms on the materials if compared to *S. oneidensis*. The latter seems to colonize all materials with less than 10% of the cells that can be seen in *G. sulfurreducens* samples. Moreover, it is hard to judge which of the materials has been covered by the most amount of cells. Hence, qPCR was established as a method to quantify cells that were bound to the anode materials.

Again, the total amount of sessile *G. sulfurreducens* cells increased with increasing available surface area (Fig. 4). On C-Tex 13 $1.05 \cdot 10^9 \pm 3.59 \cdot 10^8$ cells could be detected, whereas only 39% and 11% of this cell number were found on graphite felt and graphite foil, respectively. It is interesting to compare these cell numbers with the current density values at 41 mV obtained in the current sweep experiments. Here, C-Tex 13 was indeed the material that allowed the best performance, followed by graphite felt and graphite foil. Nevertheless, the progression of the decreasing current density values is not parallel to the decreasing cell numbers, since MFCs with graphite felt and graphite foil as anode materials showed current densities at 41 mV of 82% and 10%, respectively as compared to C-Tex 13. Hence, either the kinetics of electron transfer from cell to anode surface is hampered on C-Tex 13 compared to graphite felt and/or there is a certain percentage of physiologically inactive or less active cells on this material. A comparison of the *S. oneidensis* cell quantification with *G. sulfurreducens* verifies the impression of the FISH experiments, since graphite foil is only

populated by 31.2%, graphite felt by 1.4%, and C-Tex 13 by 11.6% of what was observed for *G. sulfurreducens*.

Standard deviations were consistently higher in the *S. oneidensis* experiments. This again indicates the importance of flavin driven electron transport for *this organism*. The cells do not have to be localized to the anode in order to thrive via extracellular electron transfer. Therefore, localization is expected to be more flexible for *S. oneidensis* compared to *G. sulfurreducens*. Of note, this might give a direction for an optimization of *S. oneidensis* strains for fuel cell applications. The aim could be to develop strains with similar biofilm producing properties as *G. sulfurreducens*. This idea was followed in experiments conducted by Lin et al. who embedded *S. oneidensis* on anodes in a PMBVF/PVA hydrogel (Lin et al., 2012). Moreover, it is known that several molecular factors are involved in biofilm formation. Hence, strain design by genetic

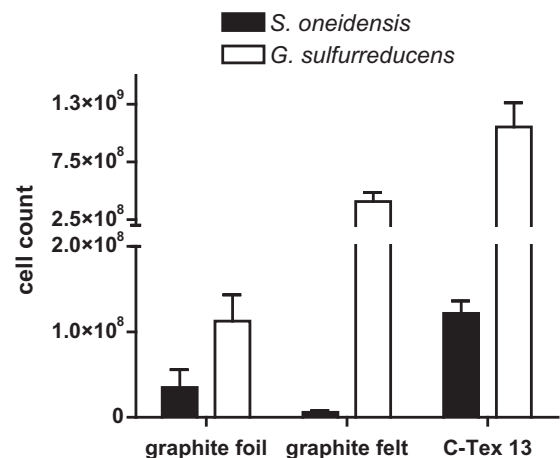


Fig. 4. Anode population. Graph displays the number of sessile *S. oneidensis* (black bars) and *G. sulfurreducens* (white bars) cells on the different materials as determined by qPCR. Experiments were conducted in triplicates. Error bars indicate standard deviation.

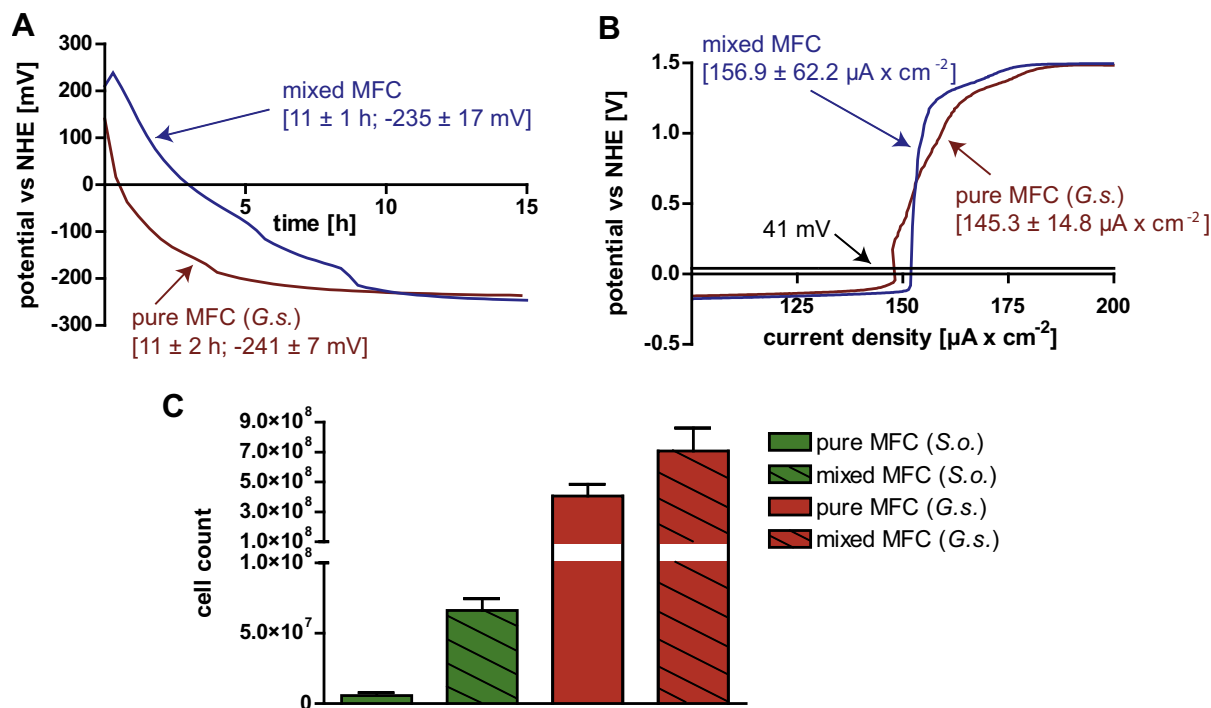


Fig. 5. Mixed MFCs. Comparison between pure culture MFCs and mixed culture MFCs (*S. oneidensis* (S.o.) and *G. sulfurreducens* (G.s.)) with graphite felt as anode material. (A) Examples of conditioning period graphs (red, *G. sulfurreducens*; blue, mixed MFC). (B) Examples of capacitance corrected current sweep graphs (red, *G. sulfurreducens*; blue, mixed MFC). (C) Comparison of sessile cells between pure culture MFCs and mixed MFCs. The number of sessile cells of *S. oneidensis* and *G. sulfurreducens* is shown in green and red, respectively. Cell numbers were determined using qPCR. Striped bars indicate the data gained from mixed MFCs. All data sets are derived from triplicates for the pure culture MFCs and quadruplicates for the mixed culture MFCs. Error bars indicate standard deviation.

manipulation would potentially offer further possibilities. These factors include for instance the Mxd-proteins involved in the production of extracellular polymeric substance (Müller et al., 2013), or the biofilm-promoting factor A (BpfA) (Theunissen et al., 2010). Overexpression of corresponding genes in a strain that is inoculated under conditions of hydrodynamic flow in MFCs could be a useful experiment to develop strains with increased exoelectrogenic performance.

Of note, graphite felt is the material that is covered with the lowest number of *S. oneidensis* cells. Nevertheless, although graphite foil is covered with more cells, it is still the material with the lowest current densities. One explanation for this finding could be that the electron transport from flavin to graphite foil is kinetically hindered. This hypothesis was already raised before based on the graphite foil potentials at the end of the conditioning period. It might arouse the question why the *S. oneidensis* cells that are bound to the graphite foil surface are not able to compensate for a potentially impaired flavin-based electron transfer. A possible answer to this question was given in a recent publication by Okamoto et al. (2013). The authors could provide evidence for a role of flavins as cofactors of outer membrane cytochromes. This is in line with crystallographic data showing possible flavin binding pockets in the structure of the outer membrane cytochrome MtrF of *S. oneidensis* (Clarke et al., 2011). Hence, if direct cell-to-surface electron transfer and shuttle-based electron transfer are both dependent on flavins, it is evident that surface bound cells would have to cope with the same limitations that occur for the electrochemical interaction with flavins and the foil material.

3.5. Performance of *S. oneidensis*/*G. sulfurreducens* mixed MFCs

So far, the interaction of isolated strains with graphite based electrode materials was analyzed. The conducted experiments revealed that *S. oneidensis* is less effective in forming biofilms. This

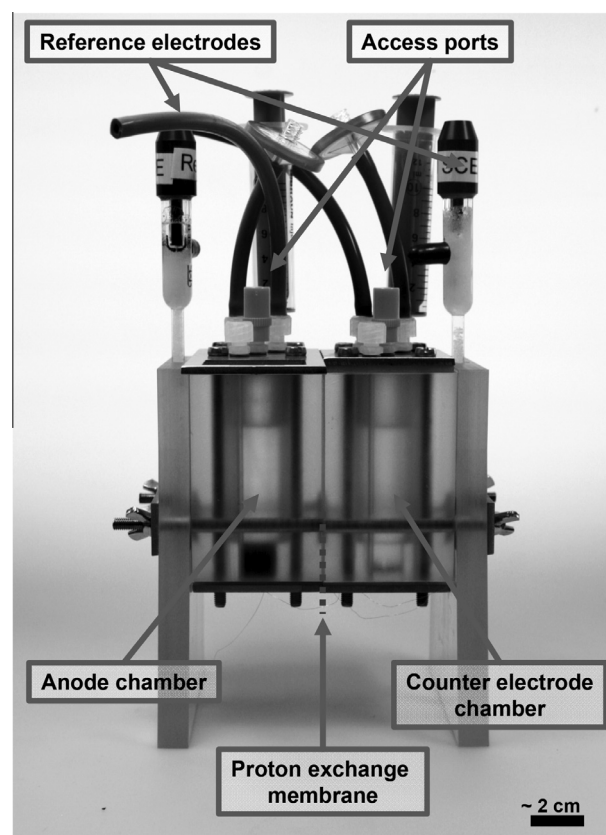


Fig. A1. MFC system. The reactor was made out of polycarbonate. Anode and cathode chambers can be separated to introduce the separator membrane.

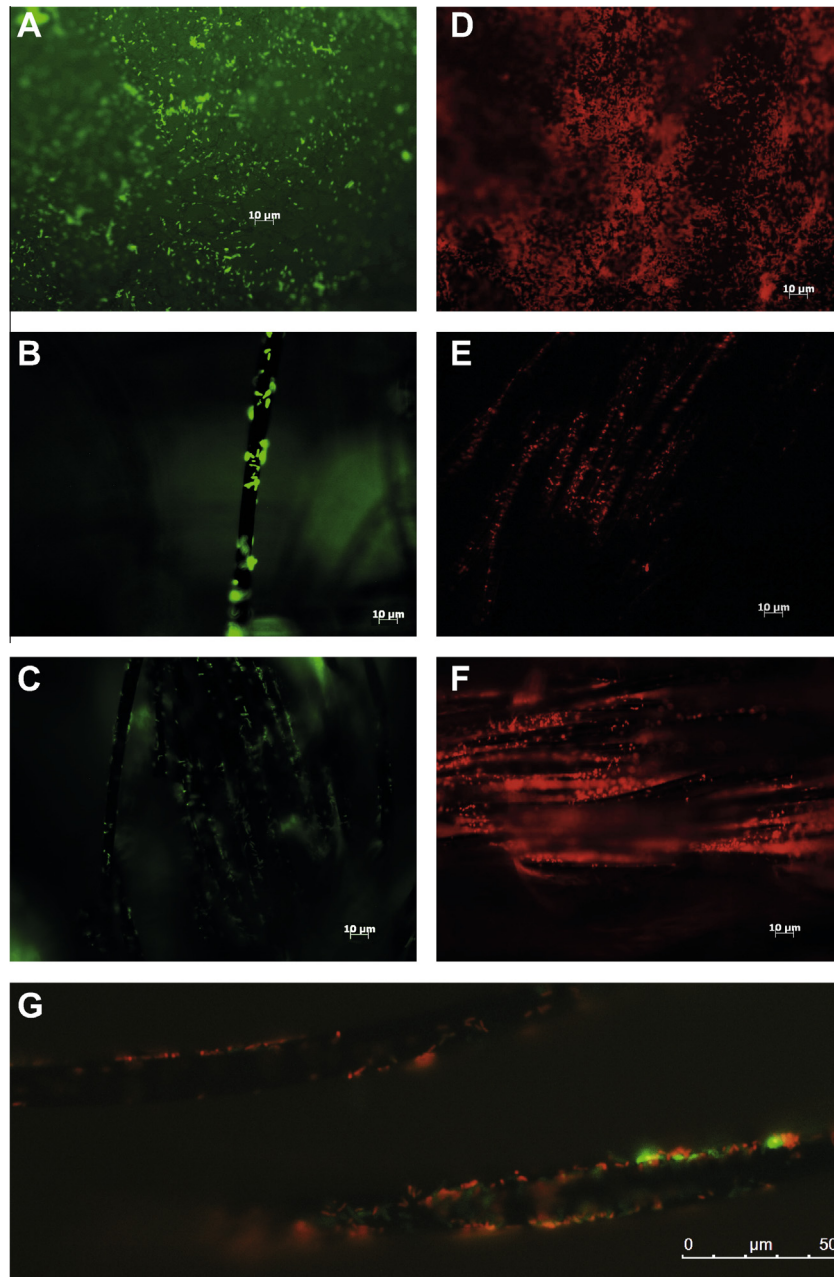


Fig. A2. Fluorescence *in situ* hybridization images of *S. oneidensis* (green) and *G. sulfurreducens* (red) cells on different anode materials as well as in mixed culture. (A–C) *S. oneidensis* biofilms on graphite foil, graphite felt, and C-Tex 13, respectively. (D–F) *G. sulfurreducens* biofilms on graphite foil, graphite felt, and C-Tex 13, respectively. (G) Mixed species biofilm of *S. oneidensis* and *G. sulfurreducens* cells on graphite felt.

seems to be compensated by its ability to use flavins as electron shuttles. A remaining question was whether a co-culture of *S. oneidensis* and *G. sulfurreducens* would show different characteristics in the established characterization routine. Co-culturing could, for instance, result in higher current densities since now the effective direct electron transfer of *G. sulfurreducens* could be combined with the use of flavins as electron shuttles. It was further unclear whether *S. oneidensis* would be detectable on the anode surface or whether this bacterium would be outcompeted by *G. sulfurreducens*. Therefore, MFCs were inoculated with a 1:1 mixture of the two proteobacteria. The conditioning period as well as the final anode potential itself were highly similar for the pure *G. sulfurreducens* culture and the co-culture, respectively [11 ± 2 h vs. 11 ± 1 h and -241 ± 7 mV vs. -235 ± 17 mV] (Fig. 5A). The capacitance corrected values of the *G. sulfurreducens* MFCs were slightly lower

than the values of the mixed MFCs [145.3 ± 14.8 vs. $156.9 \pm 62.2 \mu\text{A cm}^{-2}$] (Fig. 5B). However, the observed difference was not significant [unpaired *t*-test $p = 0.279$]. FISH revealed mixed species biofilms with a clear dominance of *G. sulfurreducens* cells (Fig. A2G), which – as determined by qPCR – accounted for 91% of the total community (Fig. 5C). Although only 9% of the biofilm consortium consisted of *S. oneidensis*, it is interesting to note that the amount of *S. oneidensis* cells was 11-fold higher than what was observed in single species experiments. Hence, it seems as if the presence of *G. sulfurreducens* leads to a higher number of sessile *S. oneidensis* cells. Furthermore, the total amount of *G. sulfurreducens* bound to the anode surface increased 1.7-fold. One possible reason for the successful interaction between *S. oneidensis* and *G. sulfurreducens* cells in anode biofilms might be that the catabolic end product of *S. oneidensis* is acetate, which is the preferred

substrate for *G. sulfurreducens*. Furthermore, growth of *S. oneidensis* is negatively affected by rising acetate concentrations (Tang et al., 2007) possibly due to a decreasing intracellular pH (Luli and Strohl, 1990). Hence, a synergistic effect might result from simultaneous acetate production and removal.

3.6. MFCs with mixed sewage

In a last series of experiments, it was the aim to evaluate whether data obtained under laboratory conditions with pure cultures of exoelectrogenic bacteria could be transferred into field experiments. In other words, the question was whether a material that was tested with superior qualities under defined laboratory conditions would also be superior if inoculated with sewage sludge. Due to the limited performance of graphite foil, only graphite felt and C-TEX 13 were used for these experiments. On graphite felt, the conditioning period step took approximately 24 h and was thereby between the values that were measured for *G. sulfurreducens* [11 ± 2 (SD) h] and *S. oneidensis* [33 ± 8 (SD) h]. The lowest potential was with -252 ± 19 (SD) mV similar to what was obtained in pure culture experiments. On C-TEX 13, 72 h were necessary to establish a constant potential of -272 ± 6 (SD) mV. Regarding current densities at 41 mV, graphite felt allows only for 3 ± 5 (SD) $\mu\text{A cm}^{-2}$, which is far below the values that could have been obtained with pure cultures. Nevertheless, also in these experiments C-TEX 13 showed better performance than graphite felt. The current density value at 41 mV of 77 ± 14 (SD) $\mu\text{A cm}^{-2}$ was even more than twofold higher compared to experiments with a pure *S. oneidensis* culture. However, it could not compete with pure cultures of *G. sulfurreducens* that allowed current densities of up to $177 \mu\text{A cm}^{-2}$.

4. Conclusions

MFC applications are dependent on stable biofilms, high current densities and short conditioning times. This combination demands compromises. Hence, the particular application will dictate whether longer conditioning times can be tolerated if current density is not enormously enhanced. Furthermore, population density cannot be directly converted into corresponding current densities, since an activity gradient runs through the anode biofilms. Hence, biofilms of a specific density will promise best efficiency. Interestingly, growth of mixed species biofilms can change the concentration of anode-attached microorganisms. This is an important implication for biotechnological processes that benefit from rigidity and stability of mixed species consortia.

Acknowledgements

Financial support by the Baden-Württemberg Stiftung under the program “Umwelttechnologieforschung” is gratefully acknowledged. Furthermore, the authors thank Elena Kipf for designing the adapted two-chamber MFC setup used in this work and photographs thereof.

Appendix A

See Figs. A1 and A2.

References

Caccavo Jr., F., Lonergan, D.J., Lovley, D.R., Davis, M., Stolz, J.F., McInerney, M.J., 1994. *Geobacter sulfurreducens* sp. nov., a hydrogen- and acetate-oxidizing dissimilatory metal-reducing microorganism. *Appl. Environ. Microbiol.* 60 (10), 3752–3759.

- Call, D.F., Logan, B.E., 2011. Lactate oxidation coupled to iron or electrode reduction by *Geobacter sulfurreducens* PCA. *Appl. Environ. Microbiol.* 77 (24), 8791–8794.
- Clarke, T.A., Edwards, M.J., Gates, A.J., Hall, A., White, G.F., Bradley, J., Reardon, C.L., Shi, L., Beliaev, A.S., Marshall, M.J., Wang, Z., Watmough, N.J., Fredrickson, J.K., Zachara, J.M., Butt, J.N., Richardson, D.J., 2011. Structure of a bacterial cell surface decaheme electron conduit. *Proc. Natl. Acad. Sci. USA* 108 (23), 9384–9389.
- Coppi, M.V., Leang, C., Sandler, S.J., Lovley, D.R., 2001. Development of a genetic system for *Geobacter sulfurreducens*. *Appl. Environ. Microbiol.* 67 (7), 3180–3187.
- Flynn, J.M., Ross, D.E., Hunt, K.A., Bond, D.R., Gralnick, J.A., 2010. Enabling unbalanced fermentations by using engineered electrode-interfaced bacteria. *MBio* 1 (5).
- Golitsch, F., Bucking, C., Gescher, J., 2013. Proof of principle for an engineered microbial biosensor based on *Shewanella oneidensis* outer membrane protein complexes. *Biosens. Bioelectron.* 47, 285–291.
- Hartshorne, R.S., Jepson, B.N., Clarke, T.A., Field, S.J., Fredrickson, J., Zachara, J., Shi, L., Butt, J.N., Richardson, D.J., 2007. Characterization of *Shewanella oneidensis* MtrC: a cell-surface decaheme cytochrome involved in respiratory electron transport to extracellular electron acceptors. *J. Biol. Inorg. Chem.* 12 (7), 1083–1094.
- Holmes, D.E., Bond, D.R., Lovley, D.R., 2004. Electron transfer by *Desulfohalobus propionicus* to Fe(III) and graphite electrodes. *Appl. Environ. Microbiol.* 70 (2), 1234–1237.
- Huggett, M.J., Crocetti, G.R., Kjelleberg, S., Steinberg, P.D., 2008. Recruitment of the sea urchin *Heliocidaris erythrogramma* and the distribution and abundance of inducing bacteria in the field. *Aquat. Microb. Ecol.* 53, 161–171.
- Kipf, E., Koch, J., Geiger, B., Erben, J., Richter, K., Gescher, J., Zengerle, R., Kerzenmacher, S., 2013. Systematic screening of carbon-based anode materials for microbial fuel cells with *Shewanella oneidensis* MR-1. *Bioresour. Technol.* 146, 386–392.
- Kloke, A., Rubenwolf, S., Bucking, C., Gescher, J., Kerzenmacher, S., Zengerle, R., von Stetten, F., 2010. A versatile miniature bioreactor and its application to bioelectrochemistry studies. *Biosens. Bioelectron.* 25 (12), 2559–2565.
- Lin, X., Nishio, K., Konno, T., Ishihara, K., 2012. The effect of the encapsulation of bacteria in redox phospholipid polymer hydrogels on electron transfer efficiency in living cell-based devices. *Biomaterials* 33 (33), 8221–8227.
- Lloyd, J.R., Leang, C., Hodges Myerson, A.L., Coppi, M.V., Cui, S., Methe, B., Sandler, S.J., Lovley, D.R., 2003. Biochemical and genetic characterization of PpcA, a periplasmic c-type cytochrome in *Geobacter sulfurreducens*. *Biochem. J.* 369 (Pt 1), 153–161.
- Logan, B.E., 2009. Exoelectrogenic bacteria that power microbial fuel cells. *Nat. Rev. Microbiol.* 7 (5), 375–381.
- Luli, G.W., Strohl, W.R., 1990. Comparison of growth, acetate production, and acetate inhibition of *Escherichia coli* strains in batch and fed-batch fermentations. *Appl. Environ. Microbiol.* 56 (4), 1004–1011.
- Marsili, E., Baron, D.B., Shikhar, I.D., Coursolle, D., Gralnick, J.A., Bond, D.R., 2008. *Shewanella* secretes flavins that mediate extracellular electron transfer. *Proc. Natl. Acad. Sci. USA* 105 (10), 3968–3973.
- Müller, J., Shukla, S., Jost, K.A., Spormann, A.M., 2013. The *mxr* operon in *Shewanella oneidensis* MR-1 is induced in response to starvation and regulated by ArcS/ArcA and BarA/UvrY. *BMC Microbiol.* 13, 119.
- Nevin, K.P., Lovley, D.R., 2000. Lack of production of electron-shuttling compounds or solubilization of Fe(III) during reduction of insoluble Fe(III) oxide by *Geobacter metallireducens*. *Appl. Environ. Microbiol.* 66 (5), 2248–2251.
- Okabe, S., Satoh, H., Watanabe, Y., 1999. In situ analysis of nitrifying biofilms as determined by *in situ* hybridization and the use of microelectrodes. *Appl. Environ. Microbiol.* 65 (7), 3182–3191.
- Okamoto, A., Hashimoto, K., Nealson, K.H., Nakamura, R., 2013. Rate enhancement of bacterial extracellular electron transport involves bound flavin semiquinones. *Proc. Natl. Acad. Sci. USA* 110 (19), 7856–7861.
- Rasband, W.S., 1997–2004. ImageJ. National Institutes of Health, Bethesda, Maryland, USA.
- Richter, H., Lanthier, M., Nevin, K.P., Lovley, D.R., 2007. Lack of electricity production by *Pelobacter carbinolicus* indicates that the capacity for Fe(III) oxide reduction does not necessarily confer electron transfer ability to fuel cell anodes. *Appl. Environ. Microbiol.* 73 (16), 5347–5353.
- Ruebush, S.S., Brantley, S.L., Tien, M., 2006. Reduction of soluble and insoluble iron forms by membrane fractions of *Shewanella oneidensis* grown under aerobic and anaerobic conditions. *Appl. Environ. Microbiol.* 72 (4), 2925–2935.
- Scott, J.H., Nealson, K.H., 1994. A biochemical study of the intermediary carbon metabolism of *Shewanella putrefaciens*. *J. Bacteriol.* 176 (11), 3408–3411.
- Tang, Y.J., Meadows, A.L., Keasling, J.D., 2007. A kinetic model describing *Shewanella oneidensis* MR-1 growth, substrate consumption, and product secretion. *Biotechnol. Bioeng.* 96 (1), 125–133.
- Theunissen, S., De Smet, L., Dansercoer, A., Motte, B., Coenye, T., Van Beeumen, J.J., Devreese, B., Savvides, S.N., Vergauwen, B., 2010. The 285 kDa Bap/RTX hybrid cell surface protein (SO4317) of *Shewanella oneidensis* MR-1 is a key mediator of biofilm formation. *Res. Microbiol.* 161 (2), 144–152.
- Yates, M.D., Kiely, P.D., Call, D.F., Rismani-Yazdi, H., Bibby, K., Peccia, J., Regan, J.M., Logan, B.E., 2012. Convergent development of anodic bacterial communities in microbial fuel cells. *ISME J.* 6 (11), 2002–2013.
- Yoon, S., Sanford, R.A., Löffler, F.E., 2013. *Shewanella* spp. use acetate as an electron donor for denitrification but not ferric iron or fumarate reduction. *Appl. Environ. Microbiol.* 79 (8), 2818–2822.